

Comprehensive Analysis of Vacancy Dynamics Due to Electromigration

H. Ceric^{*}, V. Deshpande[□], Ch. Hollauer^{*}, S. Holzer[°], T. Grasser[°], and S. Selberherr^{*}

^{*}Institute for Microelectronics, TU Vienna

Gusshausstrasse 27-29/E360, A-1040 Vienna, Austria

[□]Synopsys Switzerland LLC, Affolternstrasse 52, CH-8050 Zurich, Switzerland

[°]Christian Doppler Laboratory for TCAD in Microelectronics at the Institute for Microelectronics

Phone: +43-1-58801/36032 Fax: +43-1-58801/36099, Email: Ceric@iue.tuwien.ac.at

1. Introduction

Downscaling transistors in integrated circuits in order to achieve higher performance goes hand in hand with reducing the cross sections of interconnects. At the same time interconnects' length is increased to accommodate larger chips with increasing functionality. These tendencies make interconnects more and more sensitive to electromigration and accompanying electro-thermal and thermo-mechanical effects, which are today the main reliability issue in modern integrated circuits. Copper with its lower resistivity, higher melting point, good mechanical strength, and better electromigration bulk performance [1] has replaced aluminum as advanced metallization solution. However copper based interconnects have introduced new problems since copper electromigrates along fast diffusion paths at the interfaces to surrounding layers [2].

The main challenge in electromigration modeling and simulation is the diversity of the relevant physical phenomena. Electromigration induced material transport is also accompanied with the material transport driven by the gradients of material concentration, mechanical stress, and temperature distribution. A comprehensive, physically based analysis of electromigration for modern copper interconnect lines serves as basis for deriving sophisticated design rules which will ensure higher steadfastness of interconnects against electromigration.

The material transport driven by electromigration is most commonly modeled by the dynamics of crystal vacancies. A high concentration of vacancies indicates a site where the nucleation of an intrinsic void is very probable. The evolution of voids inside the interconnect lines is the cause of the resistance change and failure of the line.

2. Theoretical Considerations

The development of intrinsic voids, which leads to interconnect failure, goes through two distinctive phases. These phases exhibit the different influence on the operating abilities of interconnects and are based on different physical phenomena.

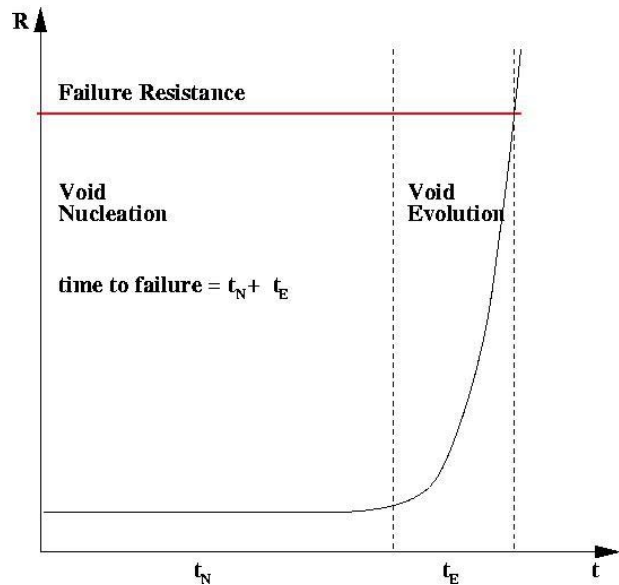


Fig. 1: Resistance behavior and failure development phases.

The first phase is the void nucleating phase in which no electromigration-generated voids are present and no significant resistance change is observable. The second phase starts when a void is nucleated and visible in SEM pictures [3]. This is the rapid phase of void development. The void expands from its initial position (nucleation site) to a size which can significantly change the resistance or completely sever the connection. If we denote with t_N the void nucleation time and with t_E the void evolution time, the time to failure t_f is then,

$$t_f = t_N + t_E \quad (1)$$

The expected resistance development during these time periods is presented in Figure 1. Depending on the interconnect layout and operating conditions, electric current Joule self-heating can induce a significant temperature gradient and thermo-mechanical stress. Electromigration induces a flux of material, which is additionally affected by the mechanical stress and temperature gradient.

In addition, volumetric strain caused by material transport is also a source of a mechanical stress field.

For a realistic description of the electromigration stressed interconnect the different diffusion paths and generation/annihilation sites of the crystal vacancies have to be considered.

3. Modeling Approach

The electromigration model applied in this work is based on propositions made in [4]. The model connects the evolution of the mechanical stress tensor with the diffusion of vacancies under full account of the influence of the geometry of the metallization.

The dynamics of the vacancies is described by the following two equations [4,11].

$$\begin{aligned} J_V &= -D_V \left(\nabla C_V + \frac{Z^* e C_V}{k_B T} \nabla \varphi + \frac{f \Omega_V C_V}{k_B T} \nabla \sigma + \frac{Q^* C_V}{k_B T^2} \nabla T \right) \\ \frac{\partial C_V}{\partial t} &= -\nabla \cdot J_V + G(C_V) \end{aligned} \quad (2)$$

C_V is the vacancy concentration, D_V is the vacancy diffusivity, $k_B T$ is the thermal energy, $Z^* e$ is the effective valence, Q^* is the heat of transport, and $G(C_V)$ is the source function which models the vacancy generation and annihilation process.

A closer look at equations (2) makes obvious that four major driving forces induce the dynamics of vacancies: the electromigration which is proportional to $\nabla \varphi$, the concentration gradient, the mechanical stress gradient

$$\nabla \sigma = 1/3 \nabla (\sigma_{11} + \sigma_{22} + \sigma_{33}), \quad (3)$$

and the temperature gradient.

If we have no residual mechanical stresses from the technological process flow and initially a uniform distribution of vacancies (what is normally the case), it is obvious that the rise of mechanical stress and concentration gradients is a response to the electromigration stressing of the interconnect material. The overall behavior of temperature gradients depends on the material choice, the geometry of the interconnect layout, and the operating conditions. Both scenarios in which temperature gradients enhance or retard vacancy transport induced by electromigration are possible.

Considering the effective vacancy diffusivity D_V we can distinguish between three basic diffusion paths and their diffusivities: bulk, grain boundaries, and copper interfaces to the other layers. Interface self-diffusion is the dominant diffusion mechanism for the case of standard barrier layers such as TiN, as shown by many experimental observations [2,3].

A vacancy generation and annihilation process, characterized by $G(C_V)$ in (2) takes places everywhere in the interconnect bulk material [4]. Some special mechanisms of vacancy recombination in the vicinity of the grain boundaries were also studied [9].

Since an atom and a vacancy have different volumes ($\Omega_V / \Omega_A = f < 1$), increasing vacancy concentration means shrinkage of the material and consequently strain is produced. This phenomena are described by the kinetic relation [4]

$$\frac{\partial \varepsilon_{kk}^V}{\partial t} = \Omega_A (f \nabla \cdot J_V + (1-f) G(C_V)) \quad (4)$$

Relation (4) clearly shows that change of the local strain ε_{kk}^V depends on the local vacancy migration $\nabla \cdot J_V$ and the recombination process $G(C_V)$.

The source of the mechanical stress during operation of an interconnect is beside electromigration itself, also a thermal mismatch between the layers of the different materials in the interconnect layout.

The material deformation induced by electromigration and thermal phenomena is described by displacement equations

$$\begin{aligned} B \left(\frac{\partial \varepsilon_{kk}^V}{\partial x_i} + \alpha \frac{\partial T}{\partial x_i} \right) &= \mu \Delta u_i + (\mu + \lambda) \frac{\partial}{\partial x_i} (\nabla \cdot \underline{u}), \\ i &= 1, 2, 3 \end{aligned} \quad (5)$$

$\underline{u} = \underline{u}(x_1, x_2, x_3)$ is the vector of displacement, λ and μ are Lamé's coefficients, B is the bulk modulus, and α is the thermal expansion coefficient.

The global transient electro-thermal behavior of the interconnect is described by the following equation system [10] for electric field potential φ , and temperature T

$$\begin{aligned} \nabla \cdot (\gamma_T \nabla T) &= c_p \rho_m \frac{\partial T}{\partial t} - \gamma_E \|\nabla \varphi\|^2 \\ \nabla \cdot (\gamma_E \nabla \varphi) &= 0 \end{aligned} \quad (6)$$

γ_E and γ_T are the thermal and the electrical conductivities, respectively, c_p is the specific heat, and ρ_m is the mass density.

The solution of equations (2-6) gives the electric potential, the temperature, displacement, and the vacancy concentration.

The model described by these equations is valid until the assumed diffusion paths dominate the material transport. When a void is nucleated, the overall material transport is dominated by material transport on the void surface and a void evolution model must be applied, e.g. the diffuse interface model [8].

The complete electromigration failure modeling is presented in Figure 2. For the numerical solution of the model equations a finite element scheme is used.

4. Results and Discussion

Focus of the investigation carried out in this work is put on an interconnect structure with six metal (copper) lines crossing four other lines at a lower level connected with vias/contacts.

The structure was generated applying a typical damascene process flow using DEP3D [5] for the deposition of the TiN barrier layer, copper, and dielectric (silicon-dioxide). For the emulation of the other deposition, etching, and polishing process steps DEVISE [7] is used.

During the operation of the interconnect a redistribution of vacancies under the influence of the various promoting factors takes place.

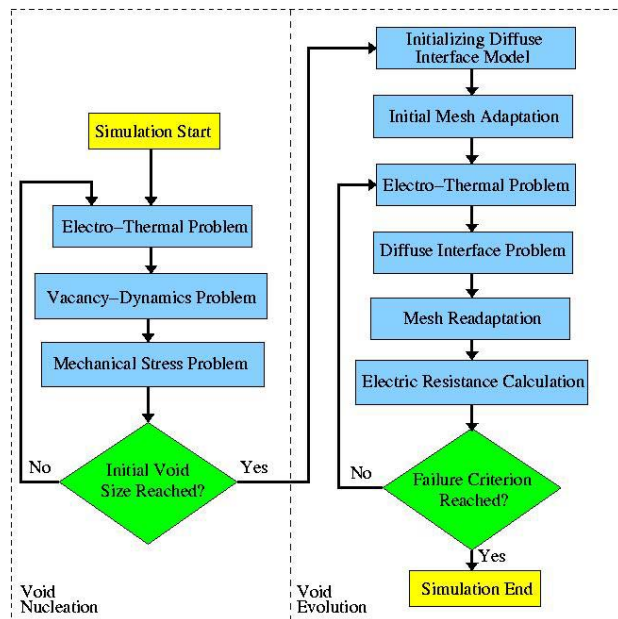


Fig. 2: Two-phase electromigration simulation scheme.

The increase of the vacancy concentration, i.e. depletion of material at specific places in interconnects metal, leads to build up of tensile stresses.

The simulated current density distribution together with the used finite element mesh is presented in Figure 3. The thermo-mechanical stress and temperature distribution are displayed in Figures 4 and 5, respectively.

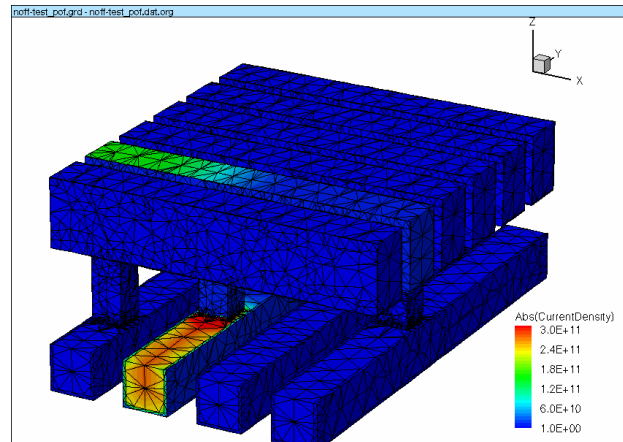


Fig. 3: Current density distribution and applied finite element mesh.

The high compressive stress in the area of the copper interconnect carrying the electrical current (Figure 4) comes from the fact that copper has a larger thermal expansion coefficient α than the TiN barrier layer. It is clear that in this case the thermal stress build up opposes the stress development due to local vacancy migration and recombination.

Starting from uniformly distributed vacancies, during the operation of the interconnect local peaks of the vacancy concentration can be observed (Figure 6). If a balance between electromigration, vacancy concentration, temperature, and mechanical stress gradients, which characterize the operating condition of the interconnect is reached, the vacancy concentration will remain at some value independent of the simulation duration: the interconnect structure is virtually immortal.

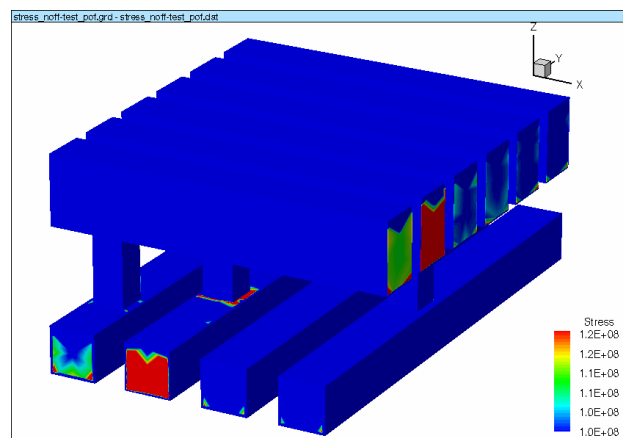


Fig. 4: Compressive stress distribution due to thermal effects.

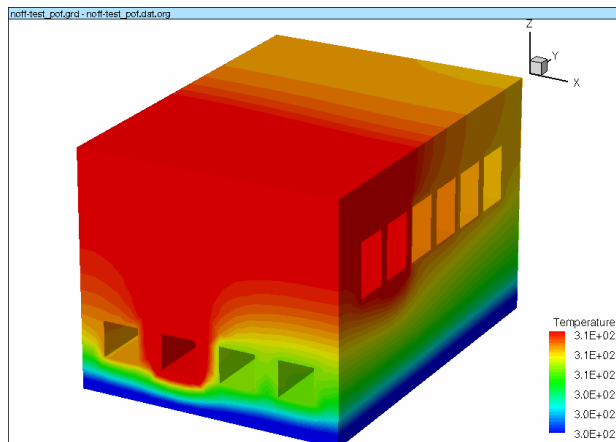


Fig. 5: Temperature distribution.

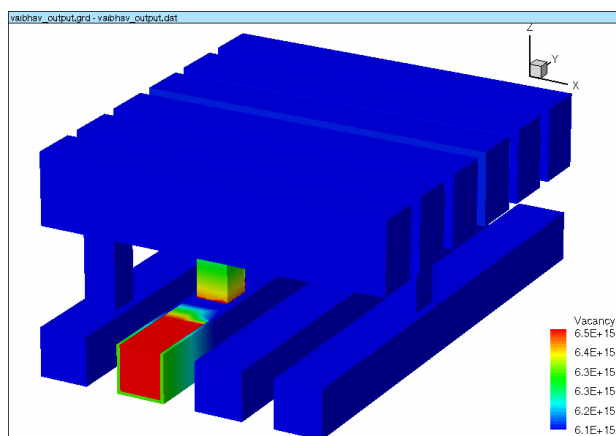


Fig. 6: Electromigration induced vacancy distribution.

However, if the electrical field is so high that electromigration overrides the material reaction presented through vacancy concentration and mechanical stress gradients, the vacancy concentration will increase steadily and at some point in time (e.g. when the vacancy concentration reaches an unrealistic high value) the applied model obviously is not valid any more. If the vacancy concentration is higher than the lattice sites' concentration throughout some volume of the macroscopic dimensions (for example 1/10 of the interconnect width), we can assume that a void is already nucleated and for any further analysis a void evolution model must be applied [8].

The interconnect layout and operating conditions chosen in the presented example produce a situation where the vacancy concentration remains stable at $6.5 \times 10^{15} \text{ cm}^{-3}$ which is well below the lattice sites concentration 10^{24} cm^{-3} .

5. Conclusion

We presented results of electromigration analysis by means of simulation for a complex interconnect structure produced by advanced process technology simulation tools. The analysis is based on a comprehensive vacancy dynamics model including all relevant driving forces accompanying electromigration. The chosen interconnect layout is resistant against electromigration failure for the applied operating conditions.

6. Acknowledgement

This work has been supported by the European Community MULSIC project IST-2000-30133.

References

- [1] C.K. Hu and J.M.E. Harper, "Copper Interconnections and Reliability," *Mater. Chem. Phys.*, vol. 52, no. 5, pp. 5-16, 1998.
- [2] S. Yokogawa, N. Okada, Y. Kakuhara, and H. Takizawa, "Electromigration Performance of Multi-Level Damascene Copper Interconnects," *Microelectron. Reliab.*, vol. 41, no. 9-10, pp. 1409-1416, 2001.
- [3] N.E. Meier, T.N. Marieb, P.A. Flinn, R.J. Gleixner, and J.C. Bravman, "In-Situ Studies of Electromigration Voiding in Passivated Copper Interconnects," *AIP Conf. Proc.*, vol. 491, no. 1, pp. 180-185, 1999.
- [4] M.E. Sarychev and Y.V. Zhitnikov, "General Model for Mechanical Stress Evolution During Electromigration," *J. Appl. Phys.*, vol. 86, no. 6, pp. 3068-3075, 1999.
- [5] E. Baer, J. Lorenz, and H. Ryssel, "Three-Dimensional Simulation of the Conformality of Copper Layers Deposited by Low-Pressure Chemical Vapor Deposition from $\text{Cu}^1(\text{tmvs})(\text{hfac})$," *Microelectron. Engin.*, vol. 50, no.1-4, pp. 481-486, 2000.
- [6] M.E. Sarychev and Y.V. Zhitnikov, "General Model for Mechanical Stress Evolution During Electromigration," *J. Appl. Phys.*, vol. 86, no. 6, pp. 3068-3075, 1999.
- [7] "DEVISE User Manual, Release 10.0," *Synopsys Switzerland Ltd.*, Switzerland, 2004.
- [8] H. Ceric and S. Selberherr, "Simulative Prediction of the Resistance Change due to Electromigration Induced Void Evolution," *Microelectron. Reliab.*, vol. 42, no. 9-11, pp. 1457-1460, 2002.
- [9] J.J. Clement, "Electromigration Modeling for Integrated Circuit Interconnect Reliability Analysis," *IEEE Trans. Dev. Mat. Reliab.*, vol. 1, no. 1, pp. 33-42.
- [10] R. Sabelka and S. Selberherr, "A Finite Element Simulator for Three-Dimensional Analysis of Interconnect Structures," *Microelectron. J.*, vol. 32, pp. 163-171, 2001.
- [11] R. Kirchheim, "Stress and Electromigration in Al-Lines of Integrated Circuits," *Acta Metallurg. Mater.*, vol. 40, no. 2, 309-323, 1992.